AN EXPERIMENTAL STUDY OF THE EFFECTS OF SOLID-TO-COOLANT THERMAL CONDUCTIVITY RATIO IN HELIUM-COOLED DIVERTOR MODULES

B. H. Mills, J. D. Rader, D. L. Sadowski, M. Yoda, S. I. Abdel-Khalik

G. W. Woodruff School of Mechanical Engineering, Georgia Institute of Technology, Atlanta, GA 30332–0405 USA
bmills@gatech.edu

As part of the ARIES study, the Georgia Tech group has experimentally studied the thermal performance of a helium-cooled 'finger-type' tungsten divertor design that uses jet impingement and a pin-fin array to cool the plasma-facing surface. These studies were performed using air at Reynolds numbers Re, spanning those for prototypical operating conditions. A brass test section heated with an oxy-acetylene torch at incident heat fluxes up to 2 MW/m^2 was used. Recently, data obtained using the same test section with room-temperature suggest that dynamic similarity between the air and helium experiments cannot be achieved by only matching Re because of the difference in the relative contributions of convection and conduction through the divertor walls. Numerical simulations suggest that achieving dynamic similarity requires matching the ratio of the thermal conductivity of the divertor module material to that of the coolant under operating conditions, as well as Re.

Studies were performed to verify that experiments at the prototypical Re and thermal conductivity ratio using helium at temperatures well below prototypical values (600 – 700°C) give Nusselt numbers Nu that are dynamically similar to those at prototypical operating conditions. Given that the thermal conductivity of helium decreases significantly as temperature decreases, matching of the thermal conductivity ratio required a test section fabricated from carbon steel, which has a thermal conductivity much lower than that of the brass alloy used in previous experiments. The resulting ratio of the test section to coolant thermal conductivities is similar to that of the tungsten alloy and helium at prototypical conditions. The data were used to develop generalized correlations for Nu, as a function of Re and the thermal conductivity ratio. The correlations can be used to determine the maximum heat flux that can be accommodated by the divertor at prototypical conditions.

I. INTRODUCTION

Several modular tungsten He-cooled divertor designs have been proposed to cool the 10 MW/m^2 heat fluxes (Ref. 1-3) expected on the divertor surface inside a fusion reactor. Designs that have been studied as part of the ARIES research program include the T-Tube,[4] the He-cooled multi-jet HEMJ (Ref. 5), the He-cooled flat plate (HCFP) (Ref. 6-7), and the He-cooled modular divertor with integrated pin array (HEMP) (Ref. 8-9). These designs rely on jet impingement, flow through a fin array, or a combination of the two using helium (He) at 10 MPa to remove this heat.

Experiments to evaluate the thermal-hydraulic performance of each design with actual materials at prototypical operating conditions are difficult and expensive due to the high temperatures and pressures required. Experiments on the HEMJ design were performed at prototypical conditions by the Karlsruhe Institute of Technology (KIT) and the Efremov Institute. These experiments focused on developing methods to fabricate the HEMJ design from the proposed materials and verifying that the design could accommodate heat fluxes of 10 MW/m^2.

Over the last several years, a number of studies to quantify and improve the thermal performance of various He-cooled divertor designs have been performed at Georgia Tech using dynamically similar experiments on brass test sections with dimensions similar to those of the actual design cooled by air at nearly ambient temperatures and pressures. The experiments were performed over a range of nondimensionalized coolant mass flow rates, or Reynolds numbers *Re*, that span the expected value at prototypical operating conditions. The outer surface of the pressure boundary of the test section was heated by an oxy-acetylene torch at heat fluxes $q'' \leq 2$ MW/m^2.

The temperature distribution over the cooled inner surface of the pressure boundary was measured by thermocouples embedded in the test section, and used to estimate nondimensional average heat transfer coefficients, or Nusselt numbers $\overline{Nu}$. The experimental data were used to develop correlations for $\overline{Nu}$ (*Re*) (assuming that the effect of Prandtl number *Pr* is minimal because the *Pr* of air and He are of the same order of magnitude). These correlations were in turn extrapolated to predict the maximum heat flux q''_{max} the design can endure without exceeding temperature limits dictated by material properties.

The pressure drop across the test section Δp was also measured, and converted to nondimensional loss coefficients K_L, which were in turn, extrapolated to prototypical conditions to predict the prototypical pressure drop, and hence the pumping power as a fraction of the incident thermal power β. Finally, these results are summarized in generalized design charts that present $q''_{\max}$ as a function of *Re* for a given maximum pressure boundary surface temperature T_s and a given β that can be used to predict how the design will perform at different operating conditions.

Recent experiments by Mills *et al.*[10] using He in a single-pass system on a modular finger-type divertor test section with dimensions similar to HEMP have shown that the $\overline{Nu}$ values determined with He are different from those obtained with air at the same *Re*. This result implied that dynamic similarity could not be achieved by only matching *Re*. Numerical simulations using ANSYS FLUENT® 13 revealed that a significant portion of the heat was being conducted through the walls of the divertor as opposed to being removed by convection at the cooled surface. The simulations also showed that the relative contributions of convection and conduction differ significantly between the He and air-cooled experiments.

By dimensional analysis, accounting for this effect introduces a new nondimensional parameter, the ratio of the thermal conductivities of the divertor module k_s and the coolant k. Re-analyzing the He and air data, as well as results from experiments performed with a third coolant, argon (Ar), to obtain correlations for $\overline{Nu}\left(Re, k_s/k\right)$ assuming a power-law dependence on both independent variables, yielded:

$$\overline{Nu} = 0.0348 Re^{0.753} \left(\frac{k_s}{k}\right)^{0.118} \quad (1)$$

The thermal conductivity ratios used to generate Eq. (1) were based on one value of k_s, namely that for brass, with $k_s/k \approx$ 900-7000. However, the thermal conductivity ratio of a W-1%La_2O_3 (WL-10) ($k_s \approx$ 116 W/(m·K) at 1000 °C) test section cooled by He ($k \approx$ 0.34 W/(m·K) at 650 °C) is much lower: $k_s/k \approx 340$.

Numerical simulations for different values of k_s and k over a range of k_s/k suggest that Eq. (1) can be extrapolated to the prototypical thermal conductivity ratio. The objective of this study was to experimentally validate that the $\overline{Nu}$ correlation of Eq. (1) at near-prototypical values of k_s/k.

Experimentally achieving $k_s/k \approx 340$ in the single-pass system using He at near-ambient temperature, and hence a value of k less than the prototypical value, requires a test section fabricated of a material with $k_s <$ 116 W/(m·K). The pressure boundary portion of the test section was therefore fabricated from AISI 1010 carbon steel, which has a thermal conductivity that varies over the range of temperatures observed in the experiments from ~63 W/(m·K) at 20 °C to ~41 W/(m·K) at 500 °C, and cooled by He, air and Ar.

The remainder of this paper is organized as follows. Section II details the experiments, while Section III presents results for $\overline{Nu}$ and K_L. Section IV discusses these results, and compares them to our previous results for the brass test section, as well as the correlation given in Eq. (1). Section V then summarizes our conclusions.

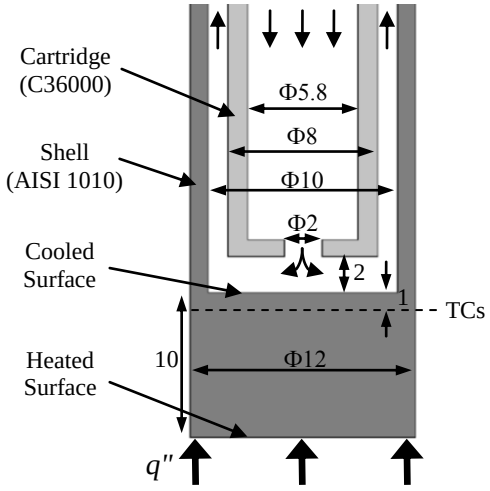

Fig. 1. A cross section of the test section. Arrows indicate coolant flow direction. All dimensions are in mm.

II. EXPERIMENT

The test section used in the experiments (Fig. 1) consisted of a cylindrical steel shell with an OD of 12 mm, ID of 10 mm, and a 10 mm thick solid tip (*i.e.*, the distance between the inner cooled and outer heated surfaces of the pressure boundary). A brass inner cylindrical cartridge with an OD of 8 mm, ID of 5.8 mm and a 3 mm thick endcap with a 2 mm diameter circular port in the center was inserted concentrically inside the steel shell; The gap between the cartridge endcap and the inner surface of the shell was 2 mm. These dimensions were similar to those of the HEMP module. Although the shell was fabricated from AISI 1010 carbon steel, the other components, including the inner cartridge, were constructed of C36000 brass alloy.

The steel shell was heated by the flame from an oxy-acetylene torch that directly impinged on the outer surface of the shell tip, or the "heated surface," at heat fluxes up to 2 MW/m^2. For the air-cooled experiments, air was supplied from the building compressed-air line at pressures up to ~0.7 MPa. The He experiments used five interconnected 300 SCF compressed-He cylinders at pressures up to ~1.4 MPa with two pressure regulators in series, while the Ar experiments used two interconnected 300 SCF compressed-Ar cylinders connected in the same manner. In all cases, the coolant entered the test section

through the inner cartridge, accelerated through the central port forming a turbulent jet that impinged on the cooled surface of the steel shell before exiting via the annular gap between the cartridge and the shell.

The coolant volumetric flow rate Q through the test section was measured using a variable-area flow meter (Brooks 1110) upstream of the test section. The coolant pressures at the flow meter and the test section inlet p_i were measured by pressure transducers (Omega PX302-2KGV and Omega PX302-300AV, respectively), and the pressure drop across the test section Δp was measured by a differential pressure transducer (Omega PX26-100DV). The coolant temperatures at the inlet and outlet of the test section T_i and T_e, respectively, were measured using Type-E thermocouple (TC) probes. Four Type-E TCs were also embedded in the steel shell tip 1 mm from the cooled surface at radial distances of 0, 1, 2, and 3 mm from the center and spaced 90° apart. Each experiment was performed at steady-state conditions, defined to be the condition where T_i and T_e varied by at most 1°C over 5 min and no heating or cooling trends were observed. All the temperatures from the embedded TCs were averaged over 200 s intervals because fluctuations in the torch flame resulted in variations as great as ~3°C.

III. RESULTS

The mass flow rate $\dot{m}$ of the coolant $\dot{m} = \rho Q$, where ρ is the coolant density at the exit of the Rotameter, was set by adjusting p_i. The non-dimensional mass flow rate $Re = 4\dot{m}/(\pi D \mu_i)$ where D = 2 mm is the diameter of the center port and μ_i is the dynamic viscosity evaluated at T_i.

The average heat flux $\overline{q''}$ incident on the test section is calculated using an energy balance assuming that heat losses to the surroundings are negligible:

$$\overline{q''} = \frac{\dot{m}\bar{c}_p (T_e - T_i)}{A_h} \tag{2}$$

where $\bar{c}_p$ is the constant-pressure specific heat evaluated at the average coolant temperature $T_{av} = (T_i + T_e)/2$ and A_h = 113.1 mm^2 is the area of the heated surface.

The embedded TC readings were extrapolated assuming 1D conduction through 1 mm of steel to estimate the temperature at the cooled surface, and these extrapolated temperatures were then averaged using an area-weighted average assuming an axisymmetric temperature distribution to determine the average cooled surface temperature $\overline{T_c}$. The average heat transfer coefficient (HTC) $\bar{h}$ over the cooled surface is then:

$$\bar{h} = \frac{\overline{q''}}{(\overline{T_c} - T_i)} \frac{A_h}{A_c} \tag{3}$$

where A_c = 78.5 mm^2 is the area of the cooled surface.

Including of the ratio between the heated and cooled surface areas in Eq. (3) assumes that all of the incident power is convected away at the cooled surface. As discussed in Mills *et al.*[10], conduction through the annular wall of the divertor can remove a significant portion of the incident heat, and this heat is ultimately convected to the coolant from the surface of the divertor side walls, and hence included in the measured average heat flux value. Finally, the nondimensional HTC, or $\overline{Nu}$ over the cooled surface is defined as follows:

$$\overline{Nu} = \frac{\bar{h} D}{k} \tag{4}$$

where k is the coolant thermal conductivity at T_{av}.

Fig. 2 summarizes the $\overline{Nu}$ results for twenty steady-state experiments: eleven with air, five with He, and four with Ar. As seen in Mills *et al.*[10], the $\overline{Nu}$ values obtained with He are significantly different from those for air and Ar. This discrepancy can be directly attributed to different fractions of the total incident power being removed at the cooled surface, as characterized by the different thermal conductivity ratios, with $k_s/k \approx 1900-2200$ for air, $2900-3000$ for Ar, and $350-380$ for He.

The measured pressure drops Δp were nondimensionalized to loss coefficients K_L:

$$K_L = \frac{\Delta p}{\rho \overline{V}^2/2} \tag{5}$$

where $\overline{V} = 4Q/(\pi D^2)$ is the average speed across the center port. Since K_L is a "hydraulic" parameter that is depends upon Re and the flow geometry, it should be independent of the material of the test section (and hence the thermal conductivity k_s). Since the flow geometry for the steel and brass test sections is identical, the correlation for $K_L(Re)$ determined from the earlier air, He and Ar results with the brass test section[10] should still be valid:

$$K_L = 8.495 \times 10^4 \, \mathrm{Re}^{-1.337} + 1.056 \tag{6}$$

Figure 3 summarizes the results of the air, He and Ar experiments with the steel test section (points), and compares them with the correlation given in Eq. (6) (line). As expected, the correlation developed for the brass test section can also be applied to these data.

IV. DISCUSSION

Figure 4 compares the experimental results shown in Figure 2 (points) with the correlation given in Eq. (1) (line) by plotting $\overline{Nu}(k_s/k)^{-0.118}$ as a function of Re. The experimental data obtained with the steel are in good agreement with the correlation, confirming that Eq. (1) is valid for $1\times10^4 < Re < 1.2\times10^5$, $350 < k_s/k < 7000$, and $0.66 < Pr < 0.72$. This correlation can therefore be used to predict the performance of He-cooled tungsten-alloy finger-type divertor modules at prototypical conditions.

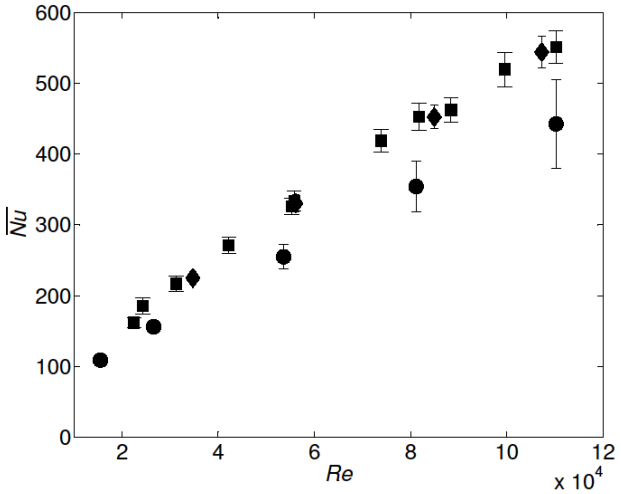

Fig. 2. $\overline{Nu}$ as a function of *Re* for the experiments performed with air (■), He (●), and Ar (♦) with the steel finger-type divertor test section. Error bars denote the experimental uncertainty.

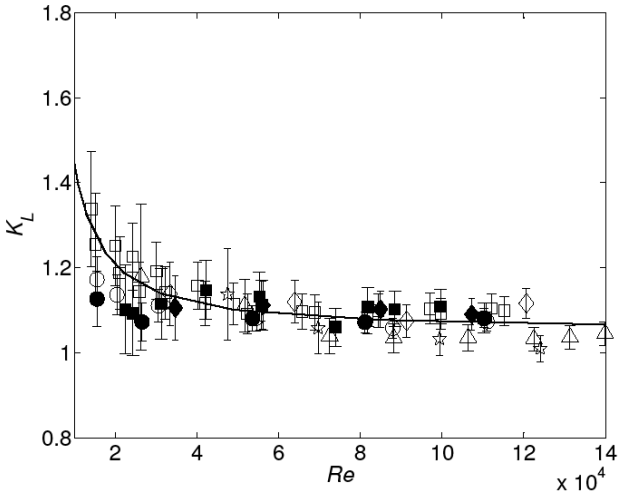

Fig. 3. K_L as a function of *Re* for the experiments performed with air (■), He (●), and Ar (♦). The new results are compared with previous results from Mills *et al.*[10] (open symbols) and correlation given by Eq. (6). Error bars denote the experimental uncertainty.

Building upon our previous numerical simulations[10], the commercial software package ANSYS FLUENT® 14 was used to analyze the experiments with the steel test section. An already existing 2D axisymmetric numerical model of a 54 mm long (axial dimension) section of the shell and tube was updated from brass to steel, with a distance of 10 mm (*vs.* 6 mm) between the cooled inner and heated outer surfaces of the shell, giving a mesh consisting of approximately 5×10^6 uniform quadrilateral cells 25 μm across. The incident heat flux was assumed to be uniform over the heated surface, and all other boundaries were assumed to be adiabatic. The simulations used the values for $\dot{m}$, T_i, p_e and $\overline{q''}$ for the experiments, and a Spalart-Allmaras turbulence model was used since previous studies[10] suggested that this turbulence model gave the most accurate results.

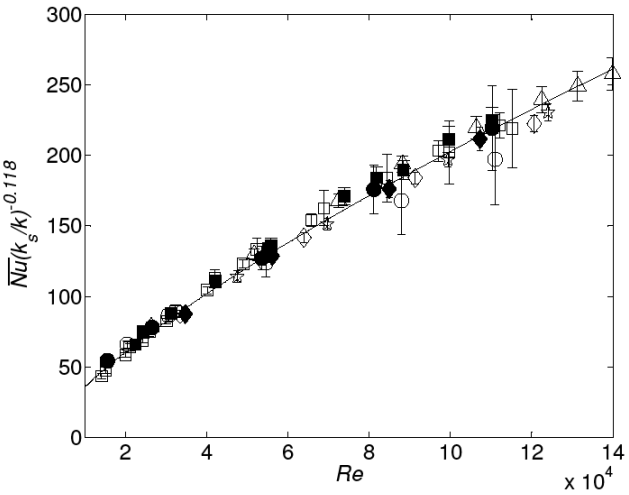

Fig. 4. Experimental data with the steel test section for air (■), He (●), and Ar (♦) compared with the correlation of Eq. (1) (line). Both are compared with the data obtained with the brass test section from Mills *et al.*[10] (open symbols). Error bars denote the experimental uncertainty.

The HTC $\bar{h}$ and $\overline{Nu}$ were calculated from the cooled surface temperatures from the simulations using Eqs. (3) and (4), respectively. Fig. 5 then shows $\overline{Nu}(k_s/k)^{-0.118}$ as a function of *Re*, and compares these numerical predictions with the correlation of Eq. (1) and the experimental results for the steel test section. The simulation results are in good agreement with the experiments and the correlation.

Finally, as detailed in Mills *et al.*[10], the simulations can also be used to estimate the fraction of the incident power removed by the coolant at the cooled surface by convection (*vs.* conducted through the walls of the divertor). Figure 6 shows this fraction, which is simply the ratio of the local heat flux integrated over the area of the cooled surface to the total thermal power incident on the heated surface $\overline{q''}A_h$, as a function of *Re*, and compares the values for the steel test section with those for the brass test section.[10]

The fraction of heat removed by convection at the cooled surface varies from ~34% to ~70% over the range of *Re* and k_s/k studied. The highest fraction of heat removed by convection was observed for the He-cooled steel test section, with the lowest $k_s/k \approx 360$ (similar to the prototypical value), while the lowest fraction was observed for the Ar-cooled brass test section with the highest $k_s/k \approx 7000$. As expected, an increase in k_s/k is associated with a decrease in the fraction of heat removed

by convection at the cooled surface, confirming that the thermal conductivity ratio can be used to characterize the relative importance of convection at the cooled surface, *vs.* conduction through the divertor walls, and that k_s/k must be included in the correlation for $\overline{Nu}$.

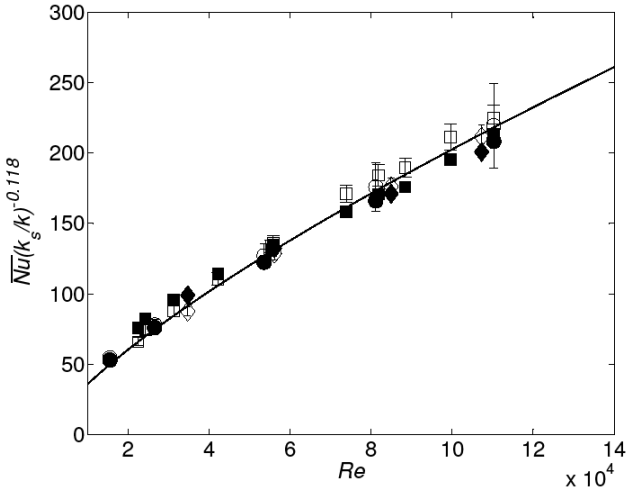

Fig. 5. Simulation results for steel test sections with air (■), He (●), and Ar (♦) compared with Eq. (1) (line) and the corresponding experimental results (open symbols). Error bars denote the experimental uncertainty.

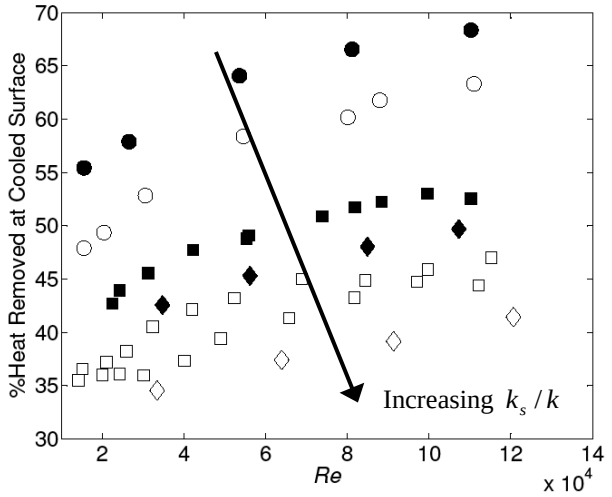

Fig. 6. Percent of incident heat removed by convection at the cooled surface found by CFD simulations for air (■), He (●), and Ar (♦). The filled and open symbols represent results for the steel and brass test sections[10], respectively. The arrow indicates increasing thermal conductivity ratio.

V. CONCLUSIONS

The effect of the ratio of the divertor and coolant thermal conductivities k_s/k on $\overline{Nu}$ at nearly prototypical values was investigated experimentally. Previous experiments using a HEMP-like divertor module fabricated in brass had developed a correlation for $\overline{Nu}$ as a function of *Re* and k_s/k, Eq. (1), for thermal conductivity ratios $900 < k_s/k < 7000$. These experiments used a nearly identical divertor module fabricated in steel cooled with helium at near-ambient temperatures to achieve the prototypical value of the thermal conductivity ratio $k_s/k \approx 340$. These dynamically similar experiments, as well as experiments using air and argon, confirmed that this correlation is valid at the prototypical thermal conductivity ratio and expanded the range. Numerical simulations of these experiments confirmed that the fraction of heat that was removed by convection at the cooled surface (*vs.* conduction through the walls of the divertor) increased as the solid-to-coolant thermal conductivity ratio decreased.

REFERENCES

1. E. DIEGELE, ET AL., "Modular He-cooled divertor for power plant application," *Fusion Engineering and Design*, **66-68**, 383 (2003).
2. P. NORAJITRA, ET AL., "Development of a helium-cooled divertor concept: design-related requirements on materials and fabrication technology," *Journal of Nuclear Materials*, **329–333**, 1594 (2004).
3. S. HERMSMEYER and S. MALANG, "Gas-cooled high performance divertor for a power plant," *Fusion Engineering and Design*, **61-62**, 197-202 (2002).
4. T. IHLI, ET AL., "Design and performance study of the helium-cooled T-Tube divertor concept," *Fusion Engineering and Design*, **82**, 249 (2007)
5. J. B. WEATHERS, ET AL., "Development of modular helium-cooled divertor for DEMO based on the multi-jet impingement (HEMJ) concept: experimental validation of thermal performance," *Fusion Engineering and Design*, **83**, 1120 (2008)
6. E. GAYTON, ET AL., "Experimental and Numerical Investigation of the Thermal Performance of the Gas-Cooled Divertor Plate Concept," *Fusion Science and Technology*, **56**, 75 (2009).
7. M. HAGEMAN, "Experimental Studies of the Thermal Performance of Gas-Cooled Plate-Type Divertors," *Fusion Sci. Technology*, **56**, 1014 (2011).
8. J. D. RADER, ET AL., "Experimental and numerical investigation of thermal performance of gas-cooled jet-impingement finger-type divertor concept," *Fusion Science and Technology*, **60**, 223 (2011)
9. B. MILLS, ET Al., "Experimental investigation of fin enhancement for gas-cooled divertor concepts," *Fusion Science and Technology*, **60**, 190 (2011)
10. B. MILLS, ET AL., "Dynamically similar studies of the thermal performance of helium-cooled finger-type divertors with and without fins," to appear in *Fusion Science and Technology*, (2012)